Iraqi Journal of Physics, 2023 *Vol.21, No. 1, PP.78-88*

https://doi.org/10.30723/ijp.v21i1.1084 *P-ISSN: 2070-4003*
E-ISSN: 2664-5548

Bandwidth Improvement of a Cone-Inverted Cylindrical and Cross Hybrids Dielectric Resonator Antennas

Nabeel Abbas Areebi[1a*] and Jamal Nasir Jabir[1b]
[1]*Department of Physics, College of Education, University of Al-Qadisiyah, Al-Diwaniyah, Iraq*
[b]Email: jamal.jabir@qu.edu.iq
[a*]Corresponding author: nabeel.alsaadawi@qu.edu.iq

Abstract

This work employs the coaxial probe method to stack and excite two cone-inverted cylindrical and cross-hybrid dielectric resonator antennas at a standard operating resonant frequency of 5.438 GHz. A drawback of these standard Dielectric Resonator Antennas (DRAs) is their narrow bandwidth. For good antenna performance, a stacked DR geometry and a thick dielectric substrate with a low dielectric constant are desired since this provides large bandwidth, better radiation power, reduces conductor loss and reduces the nonappearance of surface waves. Many approaches, such as changing the shape of the dielectric resonator, have been used to enhance bandwidth. Using DRA, which has the lowest dielectric constant, increases the bandwidth and the electromagnetic energy. In the current work, bandwidth improvement was significantly achieved by the proposed geometry by varying the antenna size. A novel hybrid DRA configuration is used to increase the bandwidth of the antenna to 89.27% and 149.23% due to cone-inverted cylindrical and cross-hybrid dielectric resonator antennas, respectively. The DRA is designed numerically via the Finite Difference Time Domain (FDTD) method. Several parameters like return loss, input impedance (verified at 50Ω) and radiation pattern are calculated. Furthermore, the stacked-hybrid technique is used to enhance the antenna's performance, which is useful for broadband communication and the demand for wireless.

Article Info.

Keywords:
Bandwidth, Dielectric Resonator Antenna, FDTD method, Hybrid Antennas, Stacked-technique.

Article history:
Received: Dec. 05, 2022
Accepted: Feb. 18, 2023
Published: Mar.01,2023

1. Introduction

An antenna is a conductor of electricity or a series of conductors used in sending or receiving systems to send or receive electromagnetic waves. A microstrip antenna is made up of two tiny superconductors with dielectric substrates in between. There are two types of microstrip antennas: the planar microstrip and the non-planar or conformal. Conformal microstrip antennas with high directivity and low cost have a wide range of applications [1]. Communications have recently developed widely, and the Dielectric Resonator Antenna (DRA) played a curial role in this due to its multitasking possibilities, which gave it many advantages in several applications. One of the most important applications is high-performance spacecraft, satellites and missiles [2].

The DRAs are distinguishable structures that offer freedom in selecting the dimensions of the dielectric material used. A wide range of dielectric permittivity (ε_r) of 6 to 100 are used in many shapes of DRA (elliptical, cylindrical, and rectangular). The attractive features of the DRA elements are high efficiency, mechanical simplicity and large bandwidth [3, 4].

One drawback of these standard DRAs is their narrow bandwidth. For a pure rectangular DRA configuration, the percentage of bandwidth (BW) up to 10% can be achieved. Several approaches have been used to improve the BW of DRA. One of these is to reduce the size of the DRA, in which the middle part of the rectangular

DRA is removed, to improve the BW by up to 28%. Modifying the geometry of the DRA into different shapes, such as a conical DRA, split cylinder and truncated tetrahedron, is another approach to enhance the bandwidth. Using U-shaped DRA, bandwidth can be increased to 72% [5].

A dual band-notched reconfigurable dielectric resonator antenna was presented by Liu et al. [6]. They showed that a rectangular dielectric resonator excited by a stepped offset microstrip feed line generated multiple resonant modes for wideband performance.

One of the methods used to enhance bandwidth is changing the shape of the dielectric resonator. Moreover, using DRA with a dielectric resonator of the lowest dielectric constant increases its bandwidth and electromagnetic (EM) energy. Increasing the bandwidth can be achieved using the multi-layer approach with different modes of excitation and different permittivities in the DRA [7].

DRAs have a much broader BW compared with a microstrip antenna. The dielectric resonator antennas (DRA) make use of radiating mode of a dielectric resonator (DR), while the microstrip antennas can be radiated only out of two narrow radiation holes. DRAs are preferable to traditional microstrip antenna because of high power handling capability, high radiation efficiency due to the absence of conductor losses, grounded planes. Avoidance of surface waves is another advantage of DRA over the microstrip antenna. However, the DR antenna and the microstrip antenna behave like resonant cavities. Other characteristics are shared between them [8].

There are several advantages of DRA; it can be integrated with Monolithic Microwave Integrated Circuit (MMIC) due to their small size. DRAs have no frequency drift with temperature variation. They can be fabricated in various shapes, such as cylindrical, hemispherical, rectangular, and cylindrical rings, and have more design flexibility. Because of the low dissipation factor of dielectric materials, DRA is a low-loss antenna. It offers high efficiency and gain because of the absence of surface wave losses and conductors. Various feeds, such as slot, coplanar lines, microstrip lines, waveguide slots, dielectric image guides and probes, can be used to excite DRA [9].

Several techniques are used to enhance bandwidth, such as multi-segment DRA, single DRA, parasitic DRA and introducing a gap between the ground plane and DRA. A bandwidth of around 10% has been achieved by a single DRA with low permittivity. Parasitic DRA introduces high gain and can improve the BW up to 17%. BW up to 20% using multi-segment DRA can be achieved. Introducing a gap between the ground plane and DRA gives a typical BW of about 30% [10, 11]. The main challenge of tactical communication systems is the accessibility of relevant information on the particular operating environment required to determine the waveform's ideal use. The propagation model focuses mainly on broadcasting and wireless communication with a high-directivity antenna [12]. It can be observed that the bandwidth percentage can be increased more than that of all the ultra-wideband hybrid DRAs listed in Table 1. A stacked DR geometry over other bandwidth enhancement techniques has several advantages: they are relatively easy to design once the design trends have been established; their radiation pattern remains reasonably constant over the 10 dB return loss bandwidth; and they can be easily accommodated into an array environment. Stacking more than one DR, such as a triple-stacked DR is possible. The success of such a configuration is very susceptible to the dielectric layers used. In fact, it has been shown to give minimum improvement over a conventional stacked DR when low dielectric constant laminates are utilized. For good antenna performance, a thick dielectric substrate having a low dielectric

constant is desired since this provides larger bandwidth, better radiation power and reduces conductor loss. The important characteristic to observe is the resonant loop created by the interaction between the two DRA. This interaction governs the achievable bandwidth. The hybrid structure is considered as the combination of a dielectric resonator antenna and another radiating resonator of the resonant feeding structure. The combined effect of DRA and parasitic elements produces wideband operation [9].

Table 1: Ultra-wideband hybrid DRAs reported in the literature.

Structure investigated	Year	Percent Bandwidth
Annular DRA excited by metal-cap loaded monopole [13]	2007	87%
Rectangular DR fed by bevel-shaped patch [14]	2011	96%
Asymmetrical T-shaped DR excited by an inverted-trapezoidal patch [15]	2012	75%
Annular column loaded cylindrical DR excited by monopole [16]	2015	56%
Three-segment composite DR fed by monopole [17]	2017	137%

1.1. Cone-Inverted Dielectric Resonator Antenna

Cone-inverted DRA can be used to prevent mode degeneracy, lower the Q factor and increase the bandwidth. The hybrid structure is the combination of a dielectric resonator antenna and another radiating resonator of the resonant feeding structure. The basic structure of cone-inverted DRA is shown in Fig. 1. The excitation was chosen by the probe feed method for several reasons, including providing a simple way to couple energy to a DRA without using a bulky feeding network, in addition to the simplicity in theoretical engineering installation and practical manufacturing. The asymmetric field distribution can be corrected using either an asymmetric DR structure or a symmetrized feeding method. The simulated coupling coefficient is reduced, using either of these two methods [18].

The ground plane of the DRA is a metal, and the dielectric cone-inverted has a dielectric constant ε_r and with height (d) and radius (a) [19]. In practical applications, the dominant mode is interesting, which has the lower resonant frequency [20].

1.2. Finite Difference Time Domain (FDTD) Method

A simulation model of the FDTD method in the time-domain is obtained by solving Maxwell curl equations. FDTD method provides an understanding of the propagation of electromagnetic waves in DRA.

Maxwell's time-dependent equations are solved in the time domain using this method by converting them to finite difference formulas. The simulation steps of the FDTD method start by representing the physical structure depending on the material type (conductor or dielectric). The second step is applying a Gaussian pulse to simulate all the sources. Then, all the fields (electric and magnetic) are calculated at any time increment. These fields are recalculated after each increment until they

decay to zero. Finally, the frequency information is extracted by Fourier transformation. Yee supposed that FDTD space is cells of an $\Delta x \Delta y \Delta z$-volume, and the components of electric and magnetic fields in 3D space are distributed, as shown in Fig. 2. Every E-field component is surrounded by four H-field components and every H-field component is surrounded by four E-field components [21].

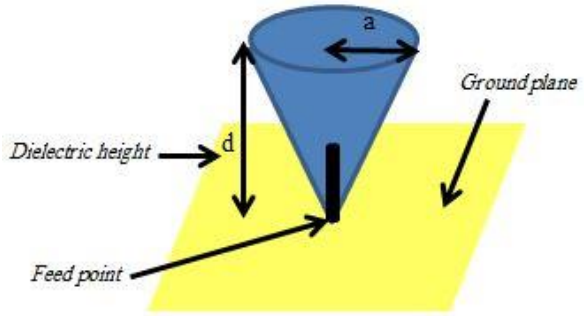

Figure 1: The geometry of cone-inverted DRA.

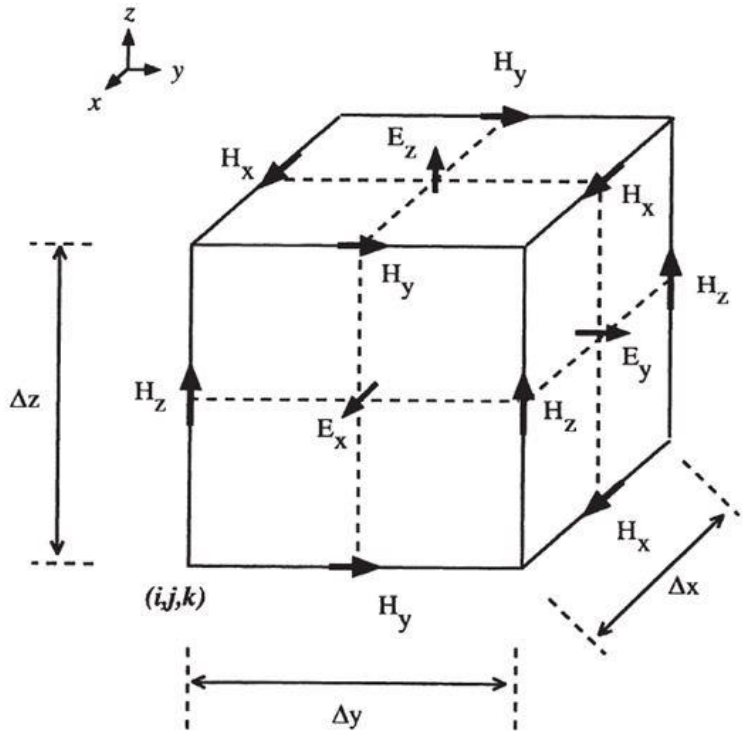

Figure 2: Yee's cell FDTD in 3D.

1.3. Basic Formulation of FDTD

Based on the system of central difference, Maxwell's curl equations can be replaced by a set of finite difference equations. The curl operator is a yield to six-coupled scalar equations which are equivalent to Maxwell's curl equations in a 3D rectangular coordinate system. These equations can be written as:

$$\frac{\partial H_x}{\partial t} = \frac{1}{\mu}\left(\frac{\partial E_y}{\partial z} - \frac{\partial E_z}{\partial y} - \rho' H_x\right) \qquad (1)$$

$$\frac{\partial H_y}{\partial t} = \frac{1}{\mu}\left(\frac{\partial E_z}{\partial x} - \frac{\partial E_x}{\partial z} - \rho' H_y\right) \quad (2)$$

$$\frac{\partial H_z}{\partial t} = \frac{1}{\mu}\left(\frac{\partial E_x}{\partial y} - \frac{\partial E_y}{\partial x} - \rho' H_z\right) \quad (3)$$

$$\frac{\partial E_x}{\partial t} = \frac{1}{\varepsilon}\left(\frac{\partial H_z}{\partial y} - \frac{\partial H_y}{\partial z} - \sigma E_x\right) \quad (4)$$

$$\frac{\partial E_y}{\partial t} = \frac{1}{\varepsilon}\left(\frac{\partial H_x}{\partial z} - \frac{\partial H_z}{\partial x} - \sigma E_y\right) \quad (5)$$

$$\frac{\partial E_z}{\partial t} = \frac{1}{\varepsilon}\left(\frac{\partial H_y}{\partial x} - \frac{\partial H_x}{\partial y} - \sigma E_z\right) \quad (6)$$

The FDTD simulation space is bounded; the radiated or scattered fields are reflected back into the simulation space at the boundary of the space.

The Perfect Matched Layer (PML) technique was presented by Berenger, who proposed an absorbing layer designed to absorb EM waves without any reflections [22]. Gauss pulse, as explained in Eq. (7), can be used to excite the system:

$$p(t) = e^{-\left(\frac{t-t_0}{\tau}\right)^2} \quad (7)$$

Where: τ represents the damping factor whose value relies on the frequency range of the problem, t_0 represents the time delay [23]. The far-field components can be obtained using the equivalence principle and through a near-field to far-field transformation.

2. Results and Discussion

2.1. Design of Cone-Inverted Dielectric Resonator Antenna

DRA is usually excited alone using a coaxial probe technique. The matching impedance and the resonance frequency can be controlled by optimizing the length and position of the feeding probe. The numerical analysis of the proposed antenna was achieved using FDTD tools.

DRA have more interesting use in wireless applications. It is a radio antenna used at microwave and millimeter frequencies that consist of a block of ceramic material [24]. In the current work, based on the detailed parametric studies, the optimized dimensions obtained for the antenna are: a standard operating resonant frequency of 5.438 GHz, the proposed DRA is with length (d) = 6 mm and radius (a) = 3.5 mm, and substrate (RT/Duroid 6010) which have a dielectric constant ($\varepsilon_{r)}$of 10.2 fixed on a ground plane of area $10 \times 10\ \text{mm}^2$. The dimensions of the proposed antenna were calculated depending on the equations presented by Al-Azza et al. [3]. The simulated and designed results of the suggested DRA configuration with the above optimum dimensions are shown in Fig. 3.

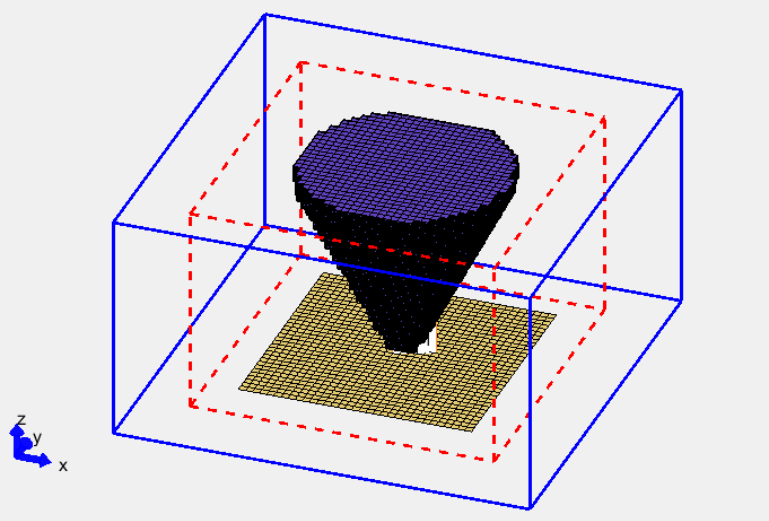

Figure 3:* The *proposed DRA calculated by FDTD method.

2.2. Resonant Frequency f_r and Input Impedance Z_{in}

For a single cone-inverted DRA, the simulation results of Z_{in} was computed. The resistance (real part) and the reactance (imaginary part) as a function of frequency were plotted, as shown in Fig. 4, at the reactance value of zero, f_r was equal to 5.438GHz and input impedance $Z_{in} = 50\Omega$. Impedance matching between transmission line and dielectric resonator antenna is essential. This matching causes maximum power transfer from the transmisssion line to the dielectric resonator antenna.

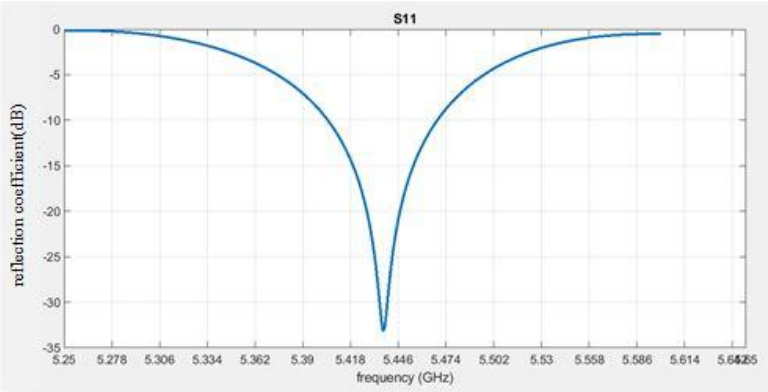

Figure 4: Input impedance versus frequency calculated by FDTD method.

2.3. Reflection coefficient or Return Loss (RL or S_{11}) and Bandwidth

A simulated input reflection coefficient of less than -10dB is illustrated in Fig. 5. As can be seen, that the calculated parameter value of S_{11} is -33 dB and the resonant frequency $f_r = 5.438$ GHz. Bandwidth is calculated from the frequency range at two sides of a -10dB return loss. The percentage bandwidth was 1.19%.

The radiation pattern or the distribution of the electric field to outer space in terms of the two planes (E and H) of the proposed optimized antenna is shown in Fig. 6, with a directivity of about 4.63 dB. Directivity can be calculated using the equations from Elsherbeni and Demir [22]. The polar representation of the field distribution in the two planes (E and H) is illustrated in Figs. 6 (a and b), respectively,

while Fig. 6(c) shows the radiation pattern in three dimensions in the two planes (E and H).

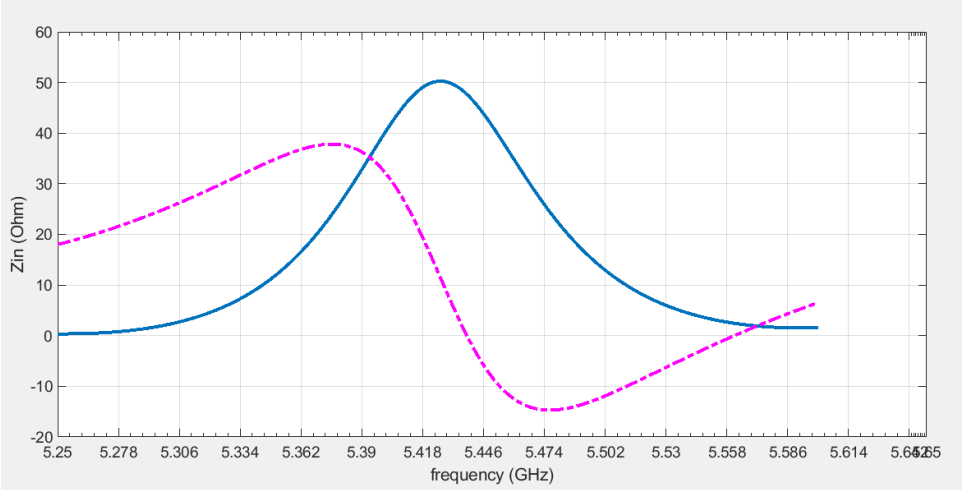

Figure 5: Return loss versus frequency calculated by FDTD method.

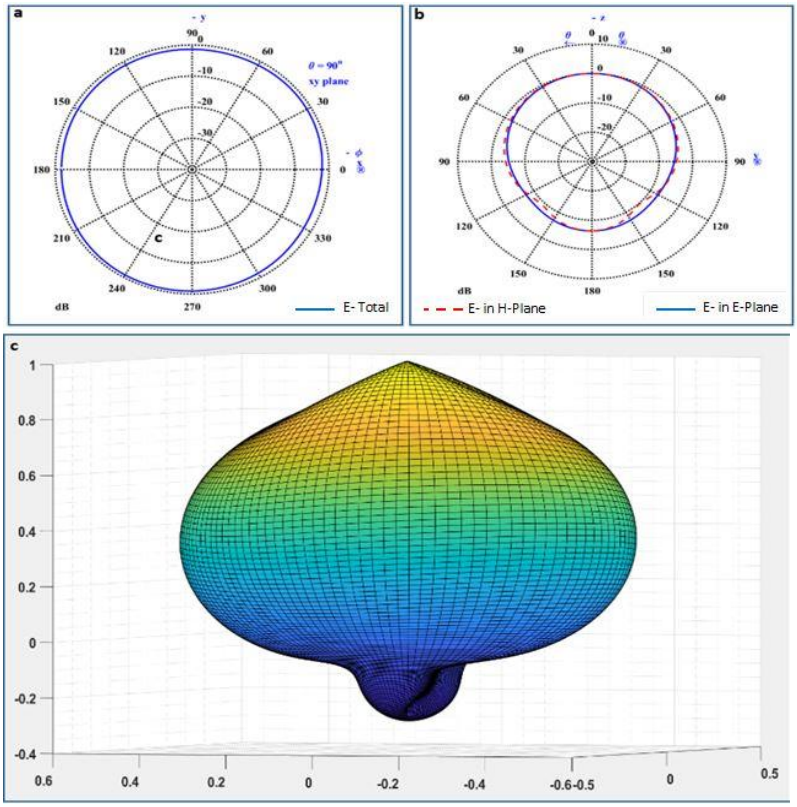

Figure 6: Radiation pattern: (a, b) in 2-D and (c) in 3-D

.

2.4. Design of Stacked Cone-Inverted Cylindrical Hybrid DRA

Multiple DRAs can be used to achieve large impedance. First, the proposed hybrid structure contains vertically stacked cone-inverted cylindrical DRAs. The proposed DRA is designed and simulated by the FDTD method. Fig. 7 shows the simulated results for stacked cone-inverted cylindrical hybrid DRA by varying the size of antenna. These two DRAs are with dielectrics of different constants. One dielectric is aluminum nitride having a dielectric constant of 8.6, and the other is RT/Duroid 6010 with a dielectric constant of 10.2. The radius and length of upper

cylindrical DRA are 3mm and 4mm, respectively. The cone-inverted DR is fed by a coaxial probe. Values of the return loss coefficients and resonant frequency are depicted in Fig. 8. It is clear from these results that there is an increase in BW from 1.19% to 89.27% compared to the single cone-inverted DRA, because the fringe fields had efficiently increased as a result of the stacked-hybrid approach, while the return loss coefficient S_{11} decreased. The resonant frequency was affected by this technique**.** Fig. 8 shows the simulated graph of the reflection coefficient of the DRA hybrid. For good antenna performance, a thick dielectric substrate having a low dielectric constant is desired since this provides larger bandwidth, better radiation power and reduces conductor loss.

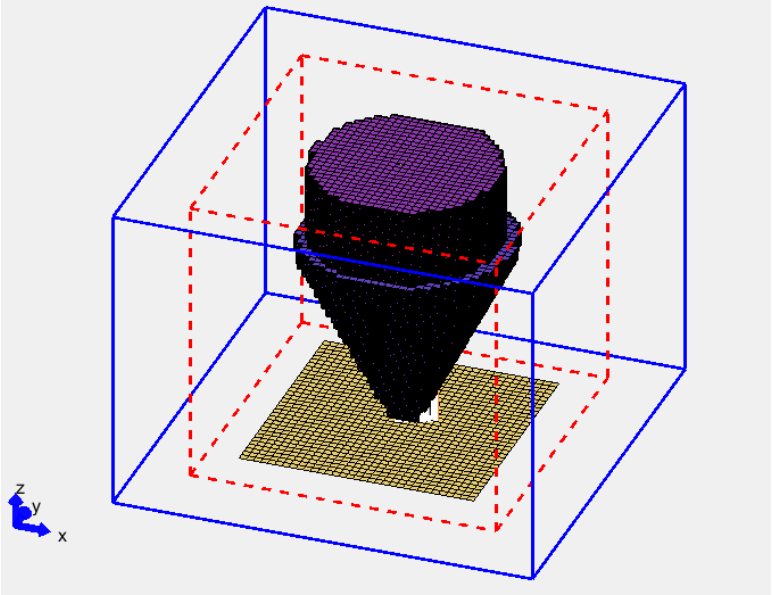

Figure 7: Stacked cone-inverted cylindrical hybrid DRA.

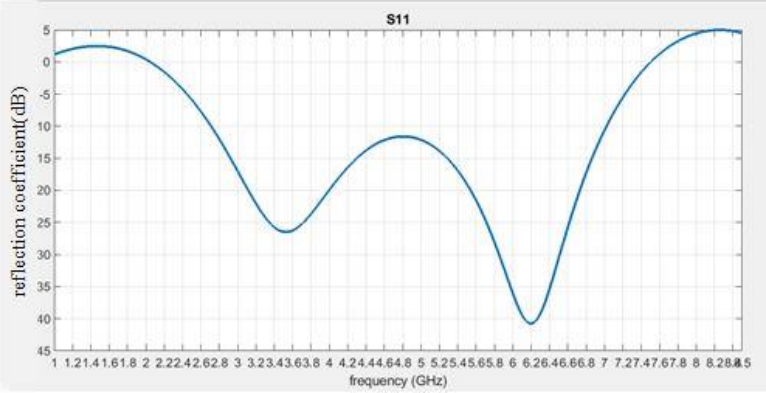

Figure 8: Return loss S_{11} for stacked cone-inverted cylindrical hybrid DRA.

2.5. Design of Stacked Cone-Inverted Cross Hybrid DRA

Another design was proposed for DRAs configuration, which is useful to broaden the impedance bandwidth, is shown in the following proposed DRAs configuration. A stacked cone-inverted cross hybrid DRAs were designed, as shown in Fig. 9. The thickness and length of cross DR are 1.5 mm and 6 mm, respectively. Moreover, the bandwidth range was enhanced, and the resonant frequency range covered was between 1.65 and 11.35 GHz with $|S_{11}| < -10$ dB. It can be observed from Fig. 10 that the bandwidth percentage increased by 149.23% more than the

entire ultra-wideband hybrid DRAs listed in Table 1. The fringe fields have a great effect on the antenna performance. Electromagnetic radiation can be produced from the created fringe fields and may provide maximum bandwidth as a result of the cross-design. It is important to mention that the amount of fringe fields depends on the antenna size as well as the height of the probe. The proposed geometry significantly improves the impedance bandwidth compared to all the earlier configurations. The hybrid structure is a combination of a dielectric resonator antenna and another radiating resonator of the resonant feeding structure. The combined effect of DRA and parasitic elements produces wideband operation. The individual bandwidth of DRA is 1.19%, while the combined bandwidth is around 150%. A significant increase in bandwidth can be achieved due to the new hybrid DRA configuration. This technique is useful for broadband communication. The asymmetric field distribution can be corrected using either an asymmetric DR structure or a symmetrized feeding method. The simulated coupling coefficient is reduced when using either of these two methods. However, the symmetric feeding method can disturb the field distribution in the DRA and thus increase the mutual coupling between these two modes.

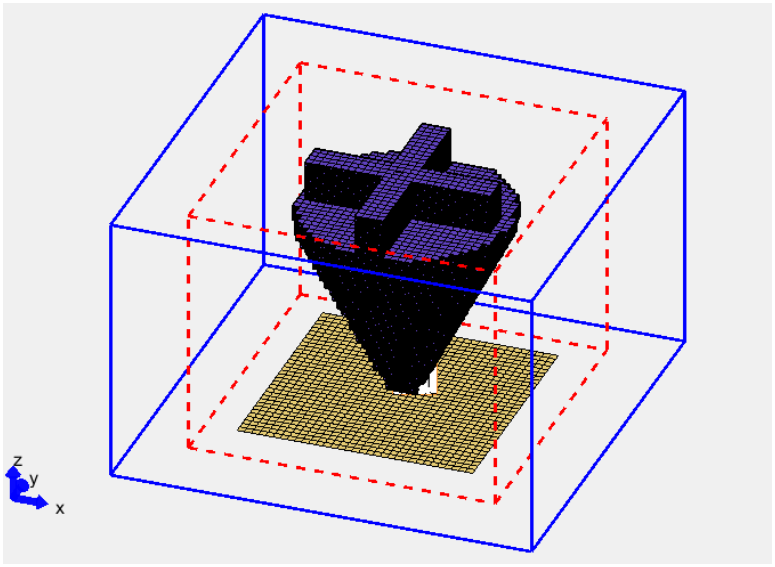

Figure 9: Stacked cone-inverted cross hybrid DRA.

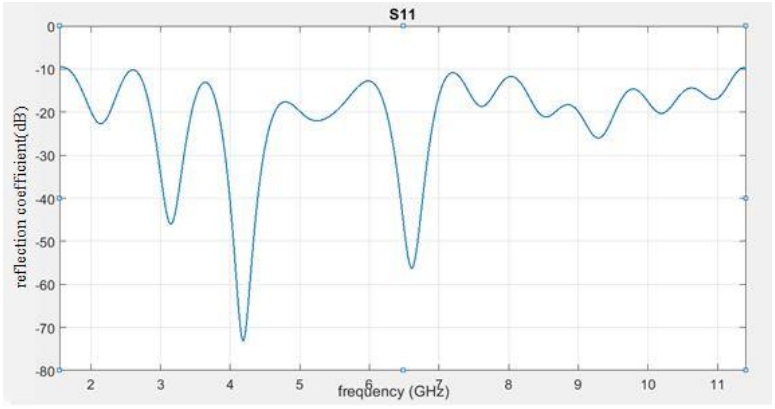

Figure 10: Return loss S_{11} for cone-inverted cross hybrid DRA.

3. Conclusions

The FDTD method was used to design and simulate stacked cone-inverted cylindrical and cross hybrid DRAs. The stacked-hybrid technique has played a vital role in enhancing DRA's performance. The coefficients of return loss were improved as a result of the two cone-inverted cylindrical and cross DRAs. Hence, this study confirmed that using the stacked-hybrid technique increases the bandwidth. For good antenna performance, a stacked DR geometry and a thick dielectric substrate with a low dielectric constant are desired since this provides a larger bandwidth, better radiation power, and reduces conductor loss.

Acknowledgements

The authors would like to thank University of Al-Qadisiyah/College of Education, Department of Physics, Ministry of Higher Education and Scientific Research of Iraq for finical support this study.

Conflict of interest

Authors declare that they have no conflict of interest.

References

1. R. J. H. O. I. J. O. T. I. Mishra, HCTL Open Inter. J. Tech. Innov. Res. **21**, 39 (2016).
2. U. E. Jallod, H. S. Mahdi, and K. M. Abood, Iraqi J. Phys. **20**, 37 (2022).
3. N. Rajasekhar, R. R. Reddy, R. Kumari, and R. Sowjanya, IEEE Indian Conference on Antennas and Propogation (InCAP) (IEEE, 2019). p. 1.
4. S. Kohar, S. Singh, and A. De, IETE J. Res., 1 (2021).
5. A. Al-Azza, N. A. Malalla, F. J. Harackiewicz, and K. Han, Prog. Electromag. Res. Lett. **79**, 79 (2018).
6. B. Liu, J. Qiu, L. Chen, and G. Li, Electronics **8**, 472 (2019).
7. H. Gharsallah, L. Osman, and L. Latrach, Microw. Opt. Tech. Lett. **59**, 1913 (2017).
8. D. Soren, R. Ghatak, R. K. Mishra, and D. Poddar, Prog. Electromag. Res. B **60**, 195 (2014).
9. S. Keyrouz and D. Caratelli, Intern. J. Anten. Propag. **2016**, 6075680 (2016).
10. S. Fakhte, H. Oraizi, and L. Matekovits, IEEE Antennas Wireless Propag. Lett. **16**, 2167 (2017).
11. H. Gharsallah, L. Osman, and L. Latrach, 2018 18th Mediterranean Microwave Symposium (MMS) (IEEE, 2018). p. 51.
12. A. L. Yusof, H. Halim, N. Ya'acob, and N. H. M. Hanapiah, Bagh. Sci. J. **18**, 1378 (2021).
13. S. Thirakoune, A. Petosa, and A. Ittipiboon, 2007 International Conference on Electromagnetics in Advanced Applications (IEEE, 2007). p. 891.
14. M. Khalily, M. K. A. Rahim, and A. A. Kishk, IEEE Antennas Wireless Propag. Lett. **10**, 393 (2011).
15. Y. Gao, Z. Feng, and L. Zhang, IEEE trans. antennas Propag. **60**, 1611 (2011).
16. Y. He, Y. Lin, C. Deng, and Z. Feng, IEEE Trans. Antennas Propag. **63**, 5874 (2015).
17. D. Guha, D. Ganguly, S. George, C. Kumar, M. Sebastian, and Y. M. Antar, IEEE Antennas Propag. Mag. **59**, 139 (2017).
18. L. Zou, Thesis, The University of Electronic Science and Technology of China, (2013).

19. G. Almpanis, C. Fumeaux, J. Frohlich, and R. Vahldieck, IEEE Antennas Wireless Propag. Lett. **8**, 279 (2008).
20. L. C. Godara, *Handbook of Antennas in Wireless Communications*. (Boca Raton, CRC press, 2018).
21. N. A. Areebi, Z. A. Ahmed, and M. M. Aubais, J. Kufa-Phys. **12**, 1 (2020).
22. E. Atef and V. Demir, *The Finite Difference Time Domain Method for Electromagnetics: With MATLAB Simulations*. 2009, Har/Cdr Edition, SciTech Publishing: North Carolina.
23. K. S. Kunz and R. J. Luebbers, *The Finite Difference Time Domain Method for Electromagnetics*. (USA, CRC press, 1993).
24. S. V. Rani, M. Sujatha, R. Surinaidu, R. V. Lakshmi, and L. Balaji, IOSR J. Elect. Commun. Eng. **11**, 61.

تحسين عرض الحزمة للهوائيات الرنينية العازلة المخروطية الشكل المقلوبة المحملة بعازل اسطواني وعازل بشكل علامة الكروس

نبيل عباس عريبي[1] , جمال ناصر جابر[1]
[1]قسم الفيزياء, كلية التربية, جامعة القادسية, الديوانية, العراق

الخلاصة

في هذا البحث, صمم هوائيين عازلين رنينيين وذلك بدمج عازل اسطواني الشكل واخرعلى شكل علامة كروس مع عازل مخروطي الشكل مقلوب ومغذى بالطريقة المحورية ليعمل بتردد رنين اساس قيمته 5.438 كيكاهيرتز. ان العيب الرئيسي للهوائيات العازلة الرنينية هو ضيق عرض الحزمة. تستخدم تقنية تكديس العوازل الرنينية التي تزيد من سمك العازل المكون للهوائي وتقلل سماحيته مما يزيد من عرض الحزمة ومن القدرة المشعة ويقلل القدرة الضائعة والموجات السطحية في الجزء الموصل. استخدمت طرائق عديدة من اجل تحسين عرض الحزمة لهذه الهوائيات كطريقة تغيير شكل العازل الرنيني. ان تقليل سماحية العازل يمكنها ان تزيد من الطاقة الكهرومغناطيسية وعرض حزمة الهوائيات الرنينية العازلة. يمكن ان نحسن عرض الحزمة بهذا التركيب الهندسي المقترح في عملنا الحالي وذلك بتغيير حجم الهوائي. ازداد عرض الحزمة الى 89.27% و 149.23% نتيجة التصميم الجديد للهوائي المخروط المقلوب والمدمج مع كل من العازل الاسطواني والعازل بشكل علامة الكروس ,على التوالي. صممت الهوائيات الرنينية العازلة عدديا باستخدام طريقة الفروق المحددة في مجال الزمن. حسبت العديد من المعاملات في العمل الحالي, منها عامل الفقد وممانعة الدخل للهوائي والتي ضبطت عند 50 اوم والهيكل الاشعاعي. علاوة على ذلك, يمكننا القول ان تقنية الدمج والتكديس يمكن ان تستخدم لتحسين اداء الهوائي من اجل تلبية متطلبات خدمات الاتصالات اللاسلكية والاتصالات التي تتطلب مدى واسع من الترددات.